PCCP

PAPER

View Article Online
View Journal | View Issue

Cite this: *Phys. Chem. Chem. Phys.*, 2014, **16**, 19206

One-step, solution-processed formamidinium lead trihalide ($FAPbI_{(3-x)}Cl_x$) for mesoscopic perovskite–polymer solar cells†

Siliu Lv,[a] Shuping Pang,*[a] Yuanyuan Zhou,[b] Nitin P. Padture,[b] Hao Hu,[a] Li Wang,[c] Xinhong Zhou,[c] Huimin Zhu,[a] Lixue Zhang,[a] Changshui Huang[a] and Guanglei Cui*[a]

Received 15th May 2014,
Accepted 7th July 2014

DOI: 10.1039/c4cp02113d

www.rsc.org/pccp

Formamidinium (FA) lead triiodide perovskite with chlorine addition ($NH_2CH{=}NH_2PbI_{(3-x)}Cl_x$) is employed as a light harvester in mesoscopic solar cells for the first time. It is demonstrated that a phase-pure $FAPbI_{(3-x)}Cl_x$ perovskite layer can be synthesized using a one-step solution-process at 140 °C, and the resultant solar cells deliver a maximum power conversion efficiency of 7.51%, which is the most efficient formamidinium-lead-halide perovskite mesoscopic solar cell employing a polymer hole-transporting layer. The effects of the thermal annealing temperature on the quality/morphology of the perovskite layer and the solar cells performance are discussed. The advantages offered by the one-step solution-processing method and the reduced bandgap make $FAPbI_{(3-x)}Cl_x$ perovskites an attractive choice for future hybrid photovoltaics.

1 Introduction

Current hybrid-photovoltaics research is driven by the need to achieve high efficiencies in low-cost solar cells.[1] This research has received a tremendous boost recently with the introduction of solution-processed organolead trihalide perovskites made from earth-abundant materials[2] as light absorbers in mesoscopic solar cells.[3–5] The power conversion efficiency (PCE or η) of perovskite-based solar cells has been climbing rapidly (>16%) owing to the excellent optical and electronic properties of the organolead trihalide perovskites such as long diffusion lengths, ultrafast carrier mobility and large absorption coefficient.[5–9] The most widely studied perovskite in this context is solution-processed methylammonium (CH_3NH_3 or MA) lead triiodide ($MAPbI_3$).[6–9] Kim *et al.*[10] were the first to use $MAPbI_3$ in solid-state mesoscopic (TiO_2) solar cells, where the perovskite layer was solution-processed using a "one-step" method. This method entailed the dissolution of PbI_2 and MAI in 1:1 (molar) in an organic solvent, which was then spin-coated and annealed to produce $MAPbI_3$ perovskite. Burschka *et al.*[11] improved the solar-cell efficiencies using a "two-step" method for the solution-processing of the $MAPbI_3$ perovskite layer, which involves sequential steps of spin-coating PbI_2 solution and drying, followed by dipping the dried PbI_2 film in a MAI solution and drying. Moreover, it has been shown that the use of $PbCl_2$, instead of PbI_2, in the precursor solution ($MAI:PbCl_2$:: 3:1 molar) results in solar cells with improved efficiencies when an identical solar-cell architecture is used.[12–14] It is not evident whether Cl^- partially substitutes for I^- in the perovskite crystal structure or the addition of $PbCl_2$ to the precursor somehow assists in the growth of more perfect perovskite layers. Thus, due to this uncertainty, and to differentiate it from $MAPbI_3$, the $MAPbI_{(3-x)}Cl_x$ nomenclature has been adopted in the literature.[12–14]

The bandgap of $MAPbI_3$-based perovskites is quite low at ~1.55 eV,[6–9] but decreasing it further can extend light absorption into the near infrared wavelengths of the solar spectrum. To that end, formamidinium (FA) lead triiodide ($FAPbI_3$) perovskite, where a relatively larger organic FA cation ($NH_2CH{=}NH_2^+$) replaces the MA cation ($CH_3NH_3^+$) in the perovskite structure, is being explored.[8,15–18] The larger FA cation results in a higher Goldschmidt tolerance factor, t, as defined for ABX_3 perovskite by[15–18] $t = [r_A + r_X]/[\sqrt{2}(r_B + r_X)]$, where r_A, r_X, and r_B are the ionic radii of the cations A (MA or FA), B (Pb) and X (I), respectively. Generally, a larger t value indicates a more symmetric perovskite crystal structure and a smaller bandgap.[15–18] In our previous study, we reported a bulk bandgap of 1.43 eV for $FAPbI_3$, and achieved a PCE of 7.50% in mesoscopic solar cells employing a P3HT polymer hole-transporting material, using a two-step solution-processing method for the deposition of the $FAPbI_3$ perovskite layer.[11] However, the use of a one-step method to solution-process the $FAPbI_3$ perovskite layer resulted in a lower PCE of 3.70% due to the non-uniformity of the resultant $FAPbI_3$ perovskite layer on mesoporous TiO_2.[16] To that end, the objective of this work was to

[a] *Qingdao Institute of Bioenergy and Bioprocess Technology, Chinese Academy of Sciences, Qingdao 266101, P. R. China. E-mail: pangsp@qibebt.ac.cn, cuigl@qibebt.ac.cn*
[b] *School of Engineering, Brown University, Providence, RI 02912, USA*
[c] *Qingdao University of Science and Technology, Qingdao 266042, P. R. China*
† Electronic supplementary information (ESI) available. See DOI: 10.1039/c4cp02113d

elucidate a more effective one-step solution-processing method entailing the use of $PbCl_2$, in place of PbI_2, in the precursor solution to deposit high quality $FAPbI_{(3-x)}Cl_x$ perovskite layers in the fabrication of mesoscopic solar cells.

In general, due the larger size of the FA cation, compared to the MA cation, the reaction leading to the one-step formation of FA-containing perovskites from a precursor solution requires a higher annealing temperature. This causes several side reactions, such as the formation of non-perovskite $FAPbI_3$ "yellow" phase, the sublimation/evaporation of FAI, and the decomposition of $FAPbI_3$, especially when the solution crystallization process is constrained within the pores of the mesostructured TiO_2. For this reason, careful control of the thermal annealing becomes even more important for producing high-quality $FAPbI_3$ phase in mesoporous TiO_2. While the effect of the annealing temperature on the one-step processing of MA-containing perovskite has been widely investigated,[19–21] the effects of thermal annealing temperature on the FA-containing perovskite layer quality/morphology, and the performance of the resulting solar cells, are studied here for the first time.

2 Experimental

2.1 Materials preparation

$NH_2CH{=}NH_2I$ (FAI) was prepared using the same method we previously reported,[16] where 3 g of formamidine acetate (99%, Aladdin Chemical Co. Ltd, China) and 8.2 g of HI (45 wt% in water) (≥45%, Sinopharm Chemical Reagent Co. Ltd, China) were mixed and reacted at 0 °C for 2 h under nitrogen atmosphere. The precipitate was collected by a rotary evaporator at 65 °C, followed by washing it with a mixture of ethanol and diethyl ether (five times) by air pump filtration. The white solid was finally dried at 60 °C under vacuum for 12 h.

The TiO_2 gel was prepared for the compact-layer deposition in the cell fabrication using the same method described in the literature.[16] Typically, 10 mL titanium(IV) isopropoxide (98%, J&K Scientific, China) was mixed with 50 mL 2-methoxyethanol (99.8%, Aladdin Chemical Co. Ltd, China) and 5 mL ethanolamine (≥99%, Sinopharm Chemical Reagent Co. Ltd, China) in a three-necked flask connected to a condenser, a thermometer, and an argon gas inlet/outlet. The mixed solution was then heated to 80 °C for 1 h with magnetic stirring, followed by heating to 120 °C for 1 h. The two-step heating stage was then repeated twice to prepare the final solution.

To prepare a 40 wt% $FAPbI_{(3-x)}Cl_x$ perovskite solution, FAI and $PbCl_2$ (Aladdin Chemical Co. Ltd, China) were mixed at a molar ratio of 3 : 1 in *N*,*N*′-dimethylformamide (DMF; Aladdin Chemical Co. Ltd, China) solution with stirring at 60 °C (30 min). A control solution without the Cl^- addition was prepared based on a 40 wt% DMF solution of PbI_2 (Aladdin Chemical Co. Ltd, China) and FAI in 1 : 1 molar ratio, resulting in a $FAPbI_3$ solution with a 40% concentration. The optimized annealing conditions for the control $FAPbI_3$ films was 160 °C for 30 min.

2.2 Solar cell fabrication

For the fabrication of the solar cells, a ~30 nm-thick, compact TiO_2 layer was spin-coated (4500 rpm, 40 s) on a patterned, fluorine-doped tin oxide (FTO) glass using the as-prepared TiO_2 gel, followed by heat-treatment at 550 °C for 30 min in air. A ~300 nm-thick TiO_2 mesoporous layer was subsequently fabricated on the TiO_2 dense layer by spin-coating (5000 rpm, 30 s) a dilute TiO_2 paste (Wuhan Geao Chemical Technology Co. Ltd, China) in ethanol (1 : 2.5 by weight). This was then sintered at 550 °C for 30 min in air. The perovskite solution was then spin-coated (5000 rpm, 60 s) on the mesoporous TiO_2 film from above. The whole substrate was then annealed in an oven at temperatures ranging from 120 °C to 170 °C for 30 min. A solution of 10 mg mL^{-1} P3HT (Sigma-Aldrich, St. Louis, MO) in 1,2-dichlorobenzene (99.5%, Aladdin Chemical Co. Ltd, China) was cast onto the perovskite coated substrate and spun at 2000 rpm for 45 s. Finally, 60 nm gold contact was thermally evaporated to complete the solar cell fabrication. All spin-coating processes were performed in a nitrogen-filled glovebox, while all the other experiments were conducted in ambient air.

2.3 Characterization

X-ray diffraction (XRD) patterns from the perovskite films were obtained using a microdiffractometer (D8-Advance, Bruker, Karlsruhe, Germany) with Cu K_α radiation (λ = 1.5406 Å) at 0.02° per step with a holding time of 10 s per step under the operation conditions of 30 kV and 40 mA. Scanning electron microscopy (SEM; S-4800, Hitachi, Japan) was performed to investigate the cross-sectional structure of the whole solar cell, and the surface morphology of the $FAPbI_{(3-x)}Cl_x$ perovskite layers. Energy dispersive spectroscopy (EDS) was performed to estimate the chlorine content of the as-deposited perovskites. The optical absorbance spectra of FTO/TiO_2/$FAPbI_{(3-x)}Cl_x$ perovskite film were measured using a UV-vis/NIR spectrophotometer (U-4100, Hitachi, Japan). Photoluminescence (PL) spectroscopy of a spin-coated $FAPbI_{(3-x)}Cl_x$ perovskite layer was performed using a spectrofluorometer (FluoroMax-4, Horiba Jobin Yvon, Japan).

The device characteristics and *J*–*V* responses of the solar cells, were measured using an analyzer (2400 Series Sourcemeter, Keithley, Cleveland, OH) under simulated AM 1.5G one sun 100 mW cm^{-2} irradiation (Oriel Sol3A Class AAA Solar Simulator, Newport Corp., Irvine, CA). The exact light intensity was calibrated using the Newport Calibrated Reference Cell and Meter with a KG3 window (Model 91150-KG3, Newport Corp., Irvine, CA). The active area of the solar cells was typically 0.09 cm^2, which is defined by the overlapping area of the FTO and gold. The *J*–*V* responses were also obtained for solar cells aged in a nitrogen atmosphere (ambient light) for 30 days.

3 Results and discussion

Fig. 1A presents a schematic representation of the perovskite structure of $FAPbI_{(3-x)}Cl_x$ showing three-dimensional PbX_3 (X = I or Cl) octahedral arrays with the FA cation ($NH_2CH{=}NH_2^+$) situated at the interstitial sites between the PbX_3 octahedra.

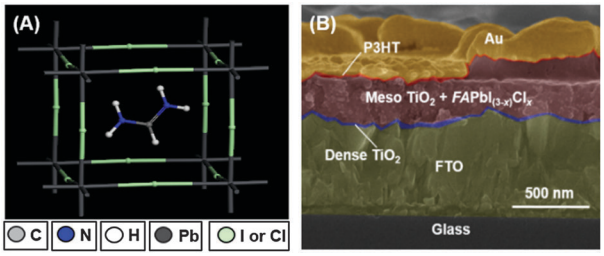

Fig. 1 (A) Structural representation of $FAPbI_{(3-x)}Cl_x$ perovskite. (B) Cross-section SEM of a typical $FAPbI_{(3-x)}Cl_x$ perovskite-based mesoscopic solar cell. The different layers (false color) are marked.

Fig. 1B shows a cross-sectional SEM image of a typical solar cell fabricated in this study. The six different layers, *i.e.* glass, FTO, dense TiO_2 blocking layer, mesoporous TiO_2 infiltrated by $FAPbI_{(3-x)}Cl_x$ perovskite (including capping layer), P3HT polymer hole transporting layer (HTL), and Au electrode are delineated using false-color enhancement. In this structure, $FAPbI_{(3-x)}Cl_x$ perovskite acts primarily as a light absorber, and to some extent as a hole transporter coupled with P3HT. The $FAPbI_{(3-x)}Cl_x$ perovskite capping layer is expected to provide good contact between the perovskite phases and the HTL, and it is particularly essential in the case of mesoscopic solar cells employing polymer HTLs as the infiltration of polymer HTLs into the mesopores is difficult.[4] Good coverage of the perovskite capping layer provides a better interface between the perovskite layer and the polymer HTL, and at the same time reduces direct contact between the HTL and TiO_2 layer. It is worth noting that although higher efficiencies are obtained in perovskite solar cells employing a spiro-OMeTAD molecular hole-transporting layer,[17,18] this layer typically requires additional processing involving long exposure to ambient atmosphere.[22] This processing step can result in the degradation of the $FAPbI_3$ perovskite layer.[22] It has been experimentally observed that $FAPbI_3$ degrades rapidly into a non-perovskite "yellow" $FAPbI_3$ phase at room temperature within 6 h of exposure to ambient air. Thus, a polymer HTL, such as P3HT, is considered to be a more robust choice for $FAPbI_3$ perovskite-based mesoscopic solar cells.

Fig. 2A presents XRD patterns of $FAPbI_{(3-x)}Cl_x$ layers on mesoporous TiO_2 annealed at different temperatures (T). Possible reactions (Rxn.) during annealing are presented in Rxns. 1–4 on the next page. A pure $FAPbI_{(3-x)}Cl_x$ perovskite layer was obtained at 140 °C for (30 min). Complete indexing of the peaks for this sample is shown in Fig. 2B, confirming the pure tetragonal $FAPbI_{(3-x)}Cl_x$ perovskite phase (space group $P3m1$, $a = b =$ 8.977(7) Å, c = 10.890(2) Å) in that layer, and the absence of any impurities. Similar to the formation of $MAPbI_{(3-x)}Cl_x$, it is suggested that a complete reaction (Rxn. 1) between the organic precursor FAI and the inorganic precursor $PbCl_2$ (FAI : $PbCl_2$::3 : 1 molar ratio) occurred; moreover, the by-product FACl was fully evaporated/sublimed (Rxn. 2). Slight c lattice parameter contraction (1.1%) is observed compared to pure $FAPbI_3$ perovskite ($a = b =$ 9.000(8) Å, c = 11.012(2) Å), which could be due to the partial substitution of the smaller Cl^- into the perovskite structure.[16,23] However, different processing conditions (*e.g.* organic component concentration in the precursor solution) were used to solution-process the $FAPbI_{(3-x)}Cl_x$ and $FAPbI_3$ layers, which makes a direct comparison difficult.[16] Detailed analytical work is underway to resolve these issues. For comparison, the XRD pattern from a corresponding optimized $FAPbI_3$ reference layer deposited using the one-step solution-processing method utilizing a pure iodine precursor solution (FAI : PbI_2::1 : 1 molar) is presented in Fig. S1 (ESI†), which shows the presence of several extraneous peaks corresponding to PbI_2 and the hexagonal non-perovskite polymorph of $FAPbI_3$ (space group $P63mc$), indicating a relatively poor quality thin film. Thus, the precursor solution using $PbCl_2$ (FAI : $PbCl_2$::3 : 1 molar ratio) enables the deposition of phase-pure perovskite layers using a one-step, solution-processing method.

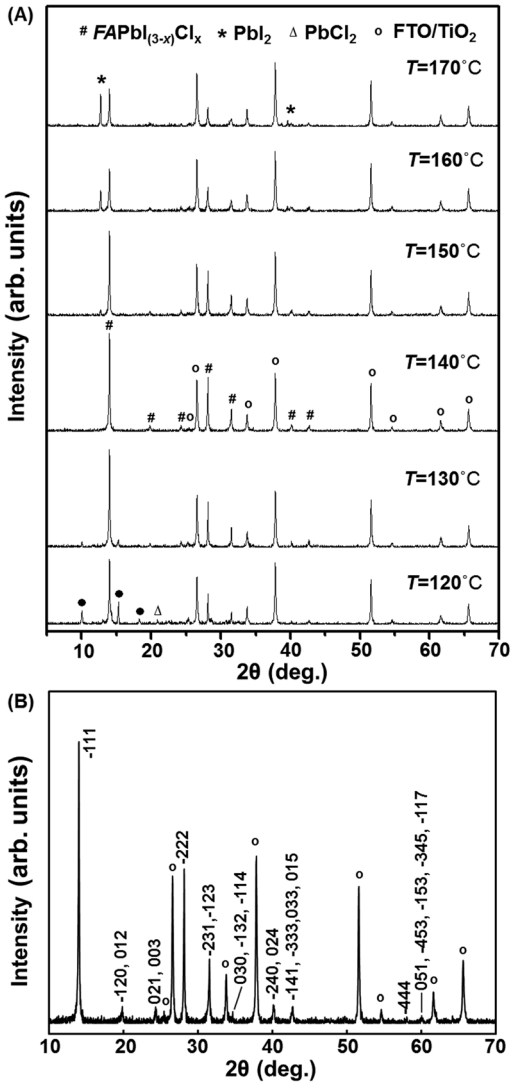

Fig. 2 (A) XRD patterns of the $FAPbI_{(3-x)}Cl_x$ layers on mesoporous TiO_2 heat-treated at (30 min): 120 °C, 130 °C, 140 °C, 150 °C, 160 °C, and 170 °C. (B) XRD pattern (140 °C) with indexed $FAPbI_{(3-x)}Cl_x$ peaks.

While pure $FAPbI_{(3-x)}Cl_x$ formation was confirmed at 140 °C, impurities were clearly observed at higher or lower annealing temperatures. At $T > 140$ °C, PbI_2 exists as the major impurity, which should be associated with fast evaporation/sublimation of

the FAI precursor (Rxn. 3) and/or the decomposition of perovskite phase (Rxn. 4). This is similar to what has been observed in the solution processing of $MAPbI_{(3-x)}Cl_x$.[8] At $T < 140$ °C, some amount of $PbCl_2$ also appears; thus, Rxn. (1) is considered to be incomplete under these conditions. However, several unidentified peaks are also shown, especially at $2\theta = 10.0°$, 15.3° and 18.4°, which probably originated from the effect of the organic component residue (FACl, FAI) in the film. The presence of organic component residue is related to the incomplete evaporation/sublimation of FACl (Rxn. 2) and the incomplete reaction between FAI and $PbCl_2$ precursors (Rxn. 1). Furthermore, DMF residue was detected in the film heat-treated at 120 °C by Fourier transform-infrared (FT-IR) spectroscopy (Fig. S2 in ESI†). DMF possibly coordinates with the unreacted $PbCl_2$, which could be responsible for the additional XRD peaks.

$$3FAI + PbCl_2 \rightarrow FAPbI_{(3-x)}Cl_x + 2FACl \quad (1)$$

$$FACl\ (solution\ or\ solid) \rightarrow FACl\ (vapour) \quad (2)$$

$$FAI\ (solution\ or\ solid) \rightarrow FAI\ (vapour) \quad (3)$$

$$FAPbI_{(3-x)}Cl_x \rightarrow FAI + PbI_2 \quad (4)$$

(Note that x is an undetermined small value.)

Fig. 3A–F show SEM images of the top surfaces of $FAPbI_{(3-x)}Cl_x$ perovskite capping layer on the mesoporous TiO_2 layer (before the deposition of P3HT) prepared using the one-step, solution-processing method as a function of the heat-treatment temperature in the range of 120–170 °C (30 min). These results show that the perovskite capping layer coverage decreases with increasing heat-treatment temperature. Better capping-layer coverage in the lower-temperature processed perovskite later appears to be related to the inclusion of organic impurities, whereas the observed shrinkage of the perovskite capping layer at higher temperatures is related to the decomposition of the perovskite phase. EDS was used to estimate the chlorine inclusion in the perovskite layer. The results in Fig. S3 (ESI†) show that the chlorine content decreases with increasing annealing temperature, and it becomes barely detectable above a heat-treatment temperature of 140 °C. This suggests that the presence of chlorine may be in form of FACl by-product, which can be more easily sublimed (Rxn. 2) at higher temperatures. Moreover, the surface of the TiO_2 nanoparticles is believed to be coated with a perovskite layer, which can be confirmed by the EDS results and the cross-sectional SEM shown in Fig. 1.

Fig. 4 presents the UV-vis-NIR absorption spectra of the deposited $FAPbI_{(3-x)}Cl_x$ layers, as a function of the annealing temperature. All the samples, especially the one heat treated at 140 °C, exhibit an absorption onset at ~835 nm, which is related to the near-IR absorption nature of $FAPbI_{(3-x)}Cl_x$. This onset is very close to the previously reported $FAPbI_3$ prepared from a pure iodine precursors solution (FAI + PbI_2 in DMF) but red-shifted compared to $MAPbI_3$ (ref. 24) and $MAPbI_{(3-x)}Cl_x$ (ref. 12) perovskites, indicating a reduced band gap when the MA cation is replaced with a FA cation. Furthermore, the appearance of a PbI_2 absorption feature at 500 nm becomes obvious in the samples heat-treated at 160 °C and 170 °C, coinciding with the large portion of PbI_2 impurity in the samples, as discussed above.[19] The presence of yellow PbI_2 in these films was also confirmed from the optical photographs in Fig. S4 (ESI†). However, the reason for the absorption features at ~480 and ~540 nm in the samples heat-treated at 120 °C and 130 °C is unclear.

In order to estimate the bandgap of $FAPbI_{(3-x)}Cl_x$, linear fits of both the absorption edge and PL emission edge were conducted, as shown in Fig. 5.[25] The estimated bandgap of $FAPbI_{(3-x)}Cl_x$ from the absorption spectrum and PL emission spectrum shows a similar value of ~1.49 eV, which is very close to the reported bandgap for $FAPbI_3$ in the literature.[15–17] The negligible change in

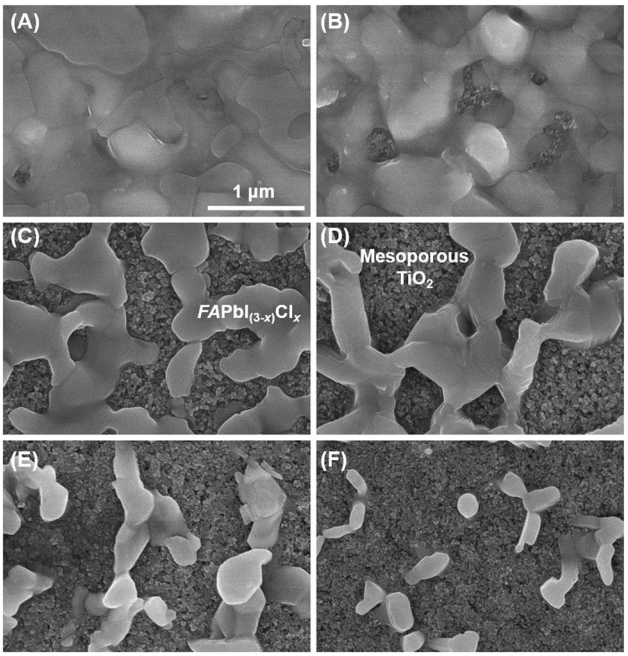

Fig. 3 SEM images of the top surfaces of the $FAPbI_{(3-x)}Cl_x$ perovskite capping layer on mesoporous TiO_2 layer heat-treated at different temperatures (30 min): (A) 120 °C, (B) 130 °C, (C) 140 °C, (D) 150 °C, (E) 160 °C, and (F) 170 °C.

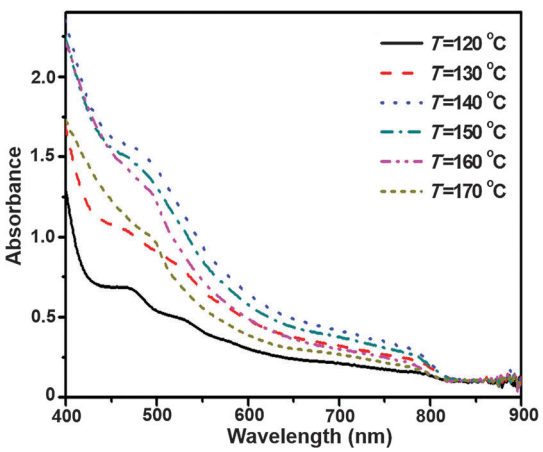

Fig. 4 UV-vis-NIR absorption spectra of the $FAPbI_{(3-x)}Cl_x$ layers on mesoporous TiO_2 heat-treated from 120 °C to 170 °C (30 min).

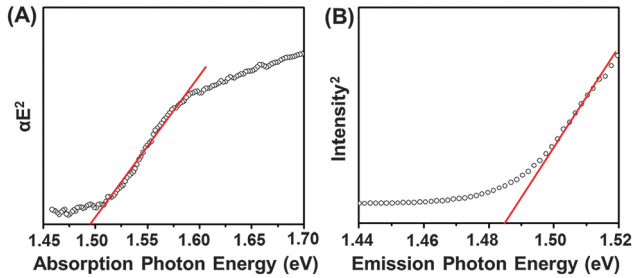

Fig. 5 (A) Linear fit of the UV-vis-NIR absorption edge for the pure $FAPbI_{3-x}Cl_x$ showing x-axis intercept of 1.492 eV; (B) linear fit of the photoluminescence (PL) emission edge for the pure $FAPbI_{3-x}Cl_x$ showing x-axis intercept of 1.485 eV. See Fig. S5 (ESI†) for the UV-vis-NIR absorption and PL spectra.

band gap between $FAPbI_{(3-x)}Cl_x$ and $FAPbI_3$ is consistent with the very small crystal structure change from XRD. Again, it indicates that only trace amounts of chlorine are present in the $FAPbI_{(3-x)}Cl_x$ crystals, which is in agreement with the EDS result. Compared to the 1.55 eV bandgap for $MAPbI_{(3-x)}Cl_x$, the bandgap of $FAPbI_{(3-x)}Cl_x$ is closer to the ideal bandgap for solar cell operation.[26]

Solar-cell performance parameters extracted from the current density (J)–voltage (V) response measurements as a function of heat-treatment temperature of the $FAPbI_{(3-x)}Cl_x$ perovskite layer are shown in Fig. 6. It is apparent that all four parameters first increase with increasing heat-treatment temperature and then decrease. This initial upward trend is attributed to the increasing phase purity of the $FAPbI_{(3-x)}Cl_x$ perovskite layer with increasing temperature. Further increases in the heat-treatment temperature results in the formation of PbI_2 beyond 140 °C. The perovskite capping layer coverage decreases monotonically with increasing temperature, which contributes to the downward trend at higher heat-treatment temperatures. Nevertheless, the maximum in the PCE (η) occurs at 140 °C heat-treatment temperature, indicating that the purity plays a dominant role in the overall solar cell performance. The maximum in J_{SC} occurs at T in the range of 140–150 °C, which also corresponds to the $FAPbI_{(3-x)}Cl_x$ perovskite with the best purity, enabling the maximum absorption of the solar spectrum under this heat-treatment condition. However, with regards to FF and V_{OC}, these parameters are influenced more by the perovskite capping-layer coverage compared with J_{SC}, and their maxima occur at T = 130 °C. The maximum V_{OC} of 0.76 V is higher than the best V_{OC} of 0.55 V in one-step, solution-processed $FAPbI_3$-based mesoscopic solar cells, and only slightly lower than that observed in the $FAPbI_3$-based mesoscopic solar cells (0.84 V) prepared using the two-step solution-processing method.[16] Although the relatively lower V_{OC} values in FA-containing perovskites solar cells is somehow related to the smaller band gap compared with the MA-containing perovskites solar cells, these results indicate that a full coverage perovskite capping layer with high purity may increase the V_{OC} of these solar cells.

Fig. 7 presents the typical current density J–V response and performance data for the solar cell (Fig. 1B) fabricated using $FAPbI_{(3-x)}Cl_x$ perovskite layer (140 °C heat-treatment) under simulated AM 1.5G one sun irradiation (100 mW cm^{-2}). This solar cell performance (η = 6.60%) is respectable as a first attempt using $FAPbI_{(3-x)}Cl_x$ perovskite. After aging the solar cell for 30 days in ambient light (inert atmosphere), its performance did not degrade, but it improved to η = 7.51%, demonstrating the stability of the $FAPbI_{(3-x)}Cl_x$ perovskite. The improvement after aging, especially the notable increase in V_{OC}, could be related to the ambient light soaking, which might improve the P3HT layer and/or the grain-coarsening in the $FAPbI_{(3-x)}Cl_x$ perovskite layer at room temperature.[27] This final maximum overall η achieved in $FAPbI_{(3-x)}Cl_x$ perovskite mesoscopic solar cells is about double the maximum (η = 3.8%) obtained using one-step solution-processed $FAPbI_3$ perovskite from the pure iodine precursor solutions (FAI + PbI_2 in DMF), and also slightly higher than the maximum η = 7.50% obtained using a more tedious, two-step, solution-processed $FAPbI_3$ perovskite.[16] Note that all these

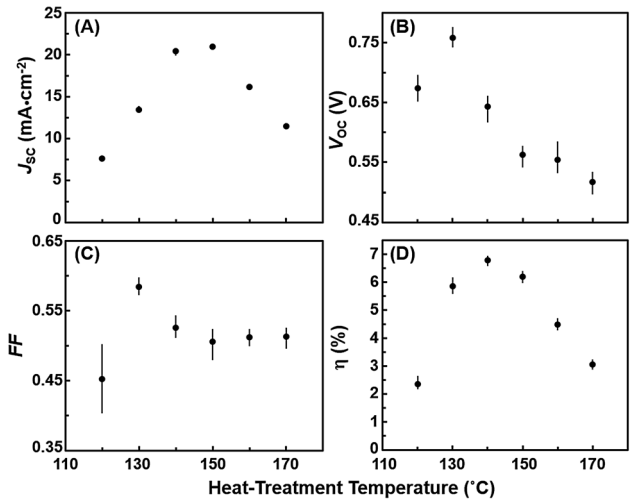

Fig. 6 Solar-cell performance parameters extracted from the J–V measurements as a function of heat-treatment temperature (120 °C to 170 °C; 30 min) of the $FAPbI_{(3-x)}Cl_x$ perovskite layers: (A) short circuit current density J_{SC}, (B) open-circuit voltage V_{OC}, (C) fill factor FF, and (D) power conversion efficiency (PCE) η.

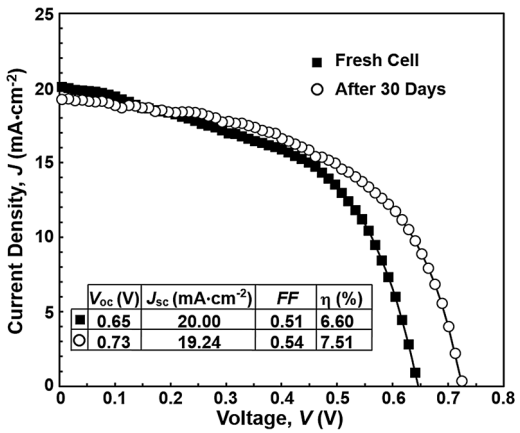

Fig. 7 J–V response and extracted performance parameters for typical freshly made and 30 days aged (in ambient light, inert atmosphere) solar cells fabricated using $FAPbI_{(3-x)}Cl_x$ perovskite (140 °C heat-treatment) under simulated AM 1.5G one sun irradiation.

comparisons are based on the same cell architecture (mesoscopic perovskite–P3HT solar cells), which directly shows the effectiveness of chlorine addition in the perovskite precursor solution for one-step processing. Like $MAPbI_{(3-x)}Cl_x$, the mechanisms responsible for the improvement in η after chlorine addition in the precursor solution in the case of $FAPbI_{(3-x)}Cl_x$ remain unclear. It is suggested that the improved uniformity of the perovskite layer could be the major contributing factor. While processing of the $FAPbI_{(3-x)}Cl_x$ perovskite layers in these solar cells was optimized for the best phase-purity, there is room for further improvement in future $FAPbI_{(3-x)}Cl_x$ perovskite–polymer photovoltaics through better perovskite capping-layer coverage and by choosing better hole transporting materials such as doped P3HT and PTAA.[28,29]

4 Conclusions

We have demonstrated, for the first time, the use of $FAPbI_{(3-x)}Cl_x$ perovskite as the light absorber in mesoscopic (TiO_2) solar cells. The use of $PbCl_2$ in the precursor solution enables a simple, one-step solution-processing method for the deposition of high-quality, stable $FAPbI_{(3-x)}Cl_x$ perovskite layers. Heat-treatment studies in the temperature range from 120 to 170 °C show that phase-pure $FAPbI_{(3-x)}Cl_x$ perovskite forms at 140 °C while the perovskite capping-layer coverage decreases with increasing temperature. Solar cells fabricated using the $FAPbI_{(3-x)}Cl_x$ perovskite layer deliver a maximum PCE of 7.51% with the P3HT polymer as the hole-transporting layer. Further optimization of the compositions, processing, and cell architecture has the potential for even higher PCEs, making $FAPbI_{(3-x)}Cl_x$ perovskites an attractive alternative to MAPb-halide-based perovskites in the rapidly expanding field of perovskite-based photovoltaics.

Acknowledgements

This research was funded by the Chinese National Natural Science Foundation (grant no. 51202266, 21271180, 21103214), the Research Program of Qingdao (13-1-4-228-jch, 13-4-1-10-gx, 12-1-4-9-(4)-jch) and the U.S. National Science Foundation (grant no. DMR-1305913).

Notes and references

1 D. S. Ginley and D. Cahen, *Fundamentals of Materials for Energy and Environmental Sustainability*, Cambridge University Press, Cambridge, 2012.
2 D. B. Mitzi, in *Progress in Inorganic Chemistry*, ed. K. D. Karlin, John Wiley & Sons, New York, 1999.
3 M. D. Mcgehee, *Nature*, 2013, **501**, 323.
4 G. Hodes, *Science*, 2013, **342**, 317.
5 R. F. Service, *Science*, 2014, **344**, 458.
6 H. J. Snaith, *J. Phys. Chem. Lett.*, 2013, **4**, 3623.
7 H. S. Kim, S. H. Im and N.-G. Park, *J. Phys. Chem. C*, 2014, **118**, 5615.
8 P. Gao, M. Grätzel and M. K. Nazeerudddin, *Energy Environ. Sci.*, 2014, **7**, 2448.
9 P. P. Boix, K. Nonomura, N. Mathews and S. G. Mhaisalkar, *Mater. Today*, 2014, **17**, 16.
10 H.-S. Kim, C.-R. Lee, J.-H. Im, K.-B. Lee, T. Moehl, A. Marchioro, S.-J. Moon, R. Humphrey-Baker, J.-H. Yum, J. E. Moser, M. Grätzel and N.-G. Park, *Sci. Rep.*, 2012, **2**, 591.
11 J. Burschka, N. Pellet, S.-J. Moon, R. Humphrey-Baker, P. Gao, M. K. Nazeeruddin and M. Grätzel, *Nature*, 2013, **499**, 316.
12 M. M. Lee, J. Teuscher, T. Miyasaka, T. N. Murakami and H. J. Snaith, *Science*, 2012, **338**, 643.
13 J. You, Z. Hong, Y. Yang, Q. Chen, M. Cai, T.-B. Song, C.-C. Chen, S. Lu, Y. Liu, H. Zhou and Y. Yang, *ACS Nano*, 2014, **8**, 1674.
14 C. Wehrenfenning, G. E. Eperon, M. B. Johnston, H. J. Snaith and L. M. Herz, *Adv. Mater.*, 2014, **26**, 1584.
15 T. M. Koh, K. Fu, Y. Fang, S. Chen, T. C. Sum, N. Mathews, S. G. Mhaisalkar, P. P. Boix and T. Baikie, *J. Phys. Chem. C*, 2014, DOI: 10.1021/JP411112K, in press.
16 S. Pang, H. Hu, J. Zhang, S. Lv, Y. Yu, F. Wei, T. Qin, H. Xu, Z. Liu and G. Cui, *Chem. Mater.*, 2014, **26**, 1485.
17 G. E. Eperon, S. D. Stranks, C. Menelaou, M. B. Johnson, L. M. Herz and H. J. Snaith, *Energy Environ. Sci.*, 2014, **7**, 982.
18 N. Pellet, P. Gao, G. Gregori, T.-Y. Yang, M. K. Nazeeruddin, J. Marer and M. Gratzel, *Angew. Chem., Int. Ed.*, 2014, **53**, 1.
19 A. Dualeh, N. Tétreault, T. Moehl, P. Gao, M. K. Nazeeruddin and M. Grätzel, *Adv. Funct. Mater.*, 2014, **24**, 3250.
20 M. Saliba, K. W. Tan, H. Sai, D. T. Moore, T. Scott, W. Zhang, L. A. Estroff, U. Wiesner and H. J. Snaith, *J. Phys. Chem. C*, 2014, DOI: 10.1021/jp500717w, in press.
21 G. E. Eperon, V. M. Burlakov, P. Docampo, A. Goriely and H. J. Snaith, *Adv. Funct. Mater.*, 2013, **24**, 151.
22 B. Cornings, L. Baeten, C. D. Dobbelaere, J. D'Haen, J. Manca and H.-G. Boyen, *Adv. Mater.*, 2013, **26**, 2041.
23 S. Colella, E. Mosconi, P. Fedeli, A. Listorti, F. Gazza, F. Orlandi, P. Ferro, T. Besagni, A. Rizzo, G. Calestani, G. Gigli, F. D. Angelis and R. Mosca, *Chem. Mater.*, 2013, **25**, 4613.
24 C. C. Stoumpos, C. D. Malliakas and G. Kanatzidis, *Inorg. Chem.*, 2013, **52**, 9019.
25 J. I. Pankove, *Optical Processes in Semiconductors*, Dover Publications, New York, 2nd edn, 2010.
26 L. L. Kazmerski, *J. Electron Spectrosc. Relat. Phenom.*, 2006, **150**, 105.
27 J.-C. Wang, C.-Y. Lu, J.-L. Hsu, M.-K. Lee, Y.-R. Hong, T.-P. Perng, S.-F. Horng and H.-F. Meng, *J. Mater. Chem.*, 2011, **21**, 5723.
28 F. D. Giacomo, S. Razza, F. Matteocci, A. D'Epifanio, S. Licoccia, T. M. Brown and A. D. Carlo, *J. Power Sources*, 2014, **251**, 152.
29 J. H. Seo, S. H. Im, J. H. Noh, T. N. Mandal, C.-S. Lim, J. A. Chang, Y. H. Lee, H.-J. Kim, A. Sarkar, M. K. Nazeeruddin, M. Grätzel and S. I. Seok, *Nat. Photonics*, 2013, **7**, 486.